













RESEARCH ARTICLE

sphingosine 1-phosphate elicits a ROS-mediated proinflammatory response in human endometrial stromal cells via ERK5 activation

Isabelle Seidita¹  | Ignazia Tusa¹  | Matteo Prisinzano¹  | Alessio Menconi¹  |
 Francesca Cencetti¹  | Silvia Vannuccini¹  | Francesca Castiglione²  |
 Paola Bruni¹  | Felice Petraglia¹  | Caterina Bernacchioni¹  |
 Elisabetta Rovida¹  | Chiara Donati¹ 

¹Department of Experimental and Clinical Biomedical Sciences “Mario Serio”, University of Florence, Florence, Italy

²Histopathology and Molecular Diagnostics, Careggi University Hospital, Florence, Italy

Correspondence

Caterina Bernacchioni and Elisabetta Rovida, Department of Experimental and Clinical Biomedical Sciences “Mario Serio”, University of Florence, viale GB Morgagni 50, 50134, Florence, Italy.

Email: caterina.bernacchioni@unifi.it and elisabetta.rovida@unifi.it

Funding information

Ente Cassa di Risparmio di Firenze (Cash Savings Institution of Florence); Fondazione AIRC per la ricerca sul cancro ETS (AIRC); Ministero dell’Istruzione, dell’Università e della Ricerca (MIUR); Università degli Studi di Firenze (UniFI)

Abstract

Endometriosis is a chronic gynecological disease affecting ~10% women in the reproductive age characterized by the growth of endometrial glands and stroma outside the uterine cavity. The inflammatory process has a key role in the initiation and progression of the disorder. Currently, there are no available early diagnostic tests and therapy relies exclusively on symptomatic drugs, so that elucidation of the complex molecular mechanisms involved in the pathogenesis of endometriosis is an unmet need. The signaling of the bioactive sphingolipid sphingosine 1-phosphate (S1P) is deeply dysregulated in endometriosis. S1P modulates a variety of fundamental cellular processes, including inflammation, neo-angiogenesis, and immune responses acting mainly as ligand of a family of G-protein-coupled receptors named S1P receptors (S1PR), S1P₁₋₅. Here, we demonstrated that the mitogen-activated protein kinase ERK5, that is expressed in endometriotic lesions as determined by quantitative PCR, is activated by S1P in human endometrial stromal cells. S1P-induced ERK5 activation was shown to be triggered by S1P_{1/3} receptors via a SFK/MEK5-dependent axis. S1P-induced ERK5 activation was, in turn, responsible for the increase of reactive oxygen species and proinflammatory cytokine expression in human endometrial stromal cells. The present findings indicate that the S1P signaling, via ERK5 activation, supports a proinflammatory response in the endometrium and establish the rationale for the exploitation of innovative therapeutic targets for endometriosis.

Abbreviations: CM-H₂DCFDA, chloromethyl-2',7'-dichlorodihydrofluorescein diacetate; DMEM, Dulbecco's modified Eagle's medium; ERK, extracellular-signal regulated kinase; ERM, ezrin, radixin, moesin; F12, Ham's F-12; GPCR, G-protein-coupled receptors; HESC, human endometrial stromal cells; MAPK, mitogen-activated protein kinase; MEF2, myocyte enhancer factor 2; NAC, N-acetyl cysteine; qPCR, quantitative polymerase chain reaction; ROS, reactive oxygen species; RSK, ribosomal S6 kinase; S1P, sphingosine 1-phosphate; S1PR, sphingosine 1-phosphate receptors; SFK, SRC family kinases; SK, sphingosine kinase; SPL, S1P lyase; Spns2, spinster homolog 2; SPP, S1P phosphatase.

Isabelle Seidita and Ignazia Tusa shared authorship.

This is an open access article under the terms of the [Creative Commons Attribution](https://creativecommons.org/licenses/by/4.0/) License, which permits use, distribution and reproduction in any medium, provided the original work is properly cited.

© 2023 The Authors. *The FASEB Journal* published by Wiley Periodicals LLC on behalf of Federation of American Societies for Experimental Biology.

KEYWORDS

bioactive sphingolipids, endometriosis, inflammation, MAPK, MAPK7, MEK5, oxidative stress, sphingosine 1-phosphate receptors, SRC family kinases

1 | INTRODUCTION

Endometriosis is a gynecological disorder defined as the presence of endometrial glands and stroma outside the uterus.^{1,2} It is a complex, estrogen-dependent, chronic, inflammatory syndrome that is estimated to affect about 10% of reproductive-age women.³ Endometriosis lacks definitive treatments because surgery and hormonal drugs are associated with high rates of symptom recurrence.^{1,4-6} Extensive investigations on the pathogenesis of this disease⁷ are showing the occurrence of complex molecular mechanisms. On the other hand, a key role of inflammation in initiation and progression of the disorder is supported by increased levels of proinflammatory cytokines in endometriotic tissue and in peritoneal fluid of patients with endometriosis.⁸⁻¹³

Sphingosine 1-phosphate (S1P) is a pleiotropic sphingolipid implicated in the regulation of many physiological as well as pathological processes including inflammation, immune response, and tumorigenesis.¹⁴ Its cellular levels are tightly regulated, depending on the relative rate between its biosynthesis and degradation.¹⁵ Most of the S1P biological actions are evoked after its extracellular release through transporters, such as spinster homolog 2 (Spns2), and by its binding to specific G-protein-coupled receptors named S1PR (S1P₁₋₅) in an autocrine/paracrine manner.¹⁶ Interestingly, S1P signaling axis has been recently reported to be altered in endometriosis,¹⁷⁻²¹ and S1P levels have been shown to be significantly augmented in the peritoneal fluid of endometriotic patients.¹⁹ Moreover, the inhibition of sphingosine kinase (SK) 1, one of the two isoenzymes responsible for S1P generation, significantly reduces the development of endometriotic lesions in an animal model of the disease.²¹ The therapeutic potential of the S1P axis has been already efficiently exploited. For instance, several S1PR selective antagonists have been developed and used in clinical settings, such as the S1P₁ antagonist KRP-203 in subacute lupus erythematosus, and the immunomodulator fingolimod, a functional antagonist of S1P_{1,3,4,5}, in multiple sclerosis and other autoimmune and inflammatory disorders.^{22,23}

The extracellular signal-related kinase 5 (ERK5) belongs to the mitogen-activated protein kinase (MAPK) family. In response to growth factors and cellular stresses, ERK5, activated by MEK5, can orchestrate gene transcription.²⁴ Like other MAPK, ERK5 can also be activated

by G-protein-coupled receptors (GPCR).^{25,26} ERK5 is involved in several biological responses, including cell survival, anti-apoptotic signaling, angiogenesis, differentiation and proliferation of several cell types.²⁴ In recent years, the ERK5 pathway has emerged as a key player in the onset and development of chronic inflammatory diseases as well as cancers, including endometrial cancer,²⁷⁻²⁹ and, with the aim to dampen the negative effects of this signaling axis, many small-molecule inhibitors of ERK5 or of its upstream activator MEK5 have been developed.

The present study evaluated the functional interaction between S1P signaling and ERK5 in human endometrial stromal cells and its effect on the inflammatory process.

2 | MATERIALS AND METHODS

2.1 | Cell culture

The immortalized human endometrial stromal cells (HESC) were purchased from American Type Culture Collection and grown in a 1:1 mixture of Dulbecco's modified Eagle's medium (DMEM) and Ham's F-12 (F12) medium, without phenol red, with 3.1 g/L glucose and 1 mM sodium pyruvate (Sigma-Aldrich, St Louis, MO, USA), supplemented with 1.5 g/L sodium bicarbonate (Sigma-Aldrich), 1% ITS+ Premix (Corning, New York, USA), 500 ng/mL puromycin and 10% charcoal-stripped fetal bovine serum (Sigma-Aldrich), at 37°C in 5% CO₂. For the experiments, cells were seeded and, the following day, serum-starved overnight in medium without serum added with 1 mg/mL fatty acid-free bovine serum albumin (BSA) (Sigma-Aldrich) before being stimulated with S1P (Sigma-Aldrich). When required, ERK5 inhibitors XMD8-92 or the more specific inhibitor of ERK5 over bromodomain-containing proteins JWG-071^{30,31} (MedChemExpress), the SFK inhibitor PP2 (MedChemExpress), the ERK1/2 inhibitor SCH772984 (MedChemExpress), the MEK5 inhibitor BIX02189 (MedChemExpress), the S1P_{1/3} antagonist VPC23019 (Avanti Polar Lipids), or the ROS scavenger N-acetyl cysteine (NAC) (Sigma-Aldrich) were administered 1 h before agonist stimulation. The effectiveness of XMD8-92 and JWG-071 at the concentration used has been reported previously^{32,33}; the ERK5 inhibitor XMD8-92 was used at concentrations with negligible off-target effects.³²

2.2 | Biological sample collection

Tissue samples were collected at Careggi University Hospital, Florence, Italy. Endometriotic lesions were from patients with endometriosis undergoing laparoscopic surgery. Control endometrial specimens were collected during diagnostic hysteroscopy (in the proliferative phase) from nonpregnant women not affected by endometriosis or other uterine disorders. The clinical and imaging investigations excluded endometriosis and other uterine disorders. All samples were histologically characterized. The endometrial cycle phase was confirmed by histologic analysis of endometrial biopsies. There was no difference in age, gravidity, and parity between the study and control groups. The patients stopped hormonal treatment at least 3 months before surgery. The institutional review board (protocol no. 13742) approved the study protocol, and all patients gave informed written consent.

2.3 | Western blot analysis

Cells were collected with the aid of a scraper and incubated for 30 min at 4°C in 50 mmol/L Tris, pH 7.5, 120 mmol/L NaCl, 6 mmol/L EGTA, 1 mmol/L EDTA, 20 mmol/L NaF, 15 mmol/L Na₄P₂O₇, 1% Nonidet, with the addition of protease inhibitor cocktail (Sigma-Aldrich) and phosphatase inhibitor cocktail (Sigma-Aldrich). They were then centrifuged for 15 min at 10000g at 4°C, and the supernatant was collected for Western blot analysis. Proteins were separated by SDS-PAGE in 6.4–9% gels and transferred onto Hybond PVDF (GE Healthcare) by electroblotting. Membranes were incubated first in PBS containing 0.1% Tween 20 and 1% BSA (blocking buffer) for 1 h at room temperature, then with primary antibody in blocking buffer overnight at 4°C. Washed membranes were incubated for 1 h at room temperature in blocking buffer containing IRDye800CW (1/20 000)-conjugated or IRDye680 (1/30 000)-conjugated secondary antibody (LI-COR Biosciences). Antibody-coated protein bands were visualized by Odyssey Infrared Imaging System Densitometry (LI-COR Biosciences). Images were quantified with ImageJ software. The following antibodies were used: rabbit polyclonal anti ERK5 (Cat #3372, [RRID:AB_330491](#)), rabbit polyclonal anti phospho-ERK5-T218/Y220 (Cat #3371, [RRID:AB_2140424](#)), rabbit polyclonal anti phospho-p90RSK-S380 (Cat #9341, [RRID:AB_330753](#)), rabbit polyclonal anti phospho-Ezrin (T567)/Radixin (T564)/Moesin (T558) (pERM, Cat# 3141, [RRID:AB_330232](#)) or rabbit polyclonal anti phospho-ERK1/2-T202/Y204 (Cat #9101, [RRID:AB_331646](#)) from Cell Signaling Technology (Danvers, MA, USA); rabbit polyclonal anti phospho-MEK5-S311/T315 (Cat#

sc-135702, [RRID:AB_2141255](#)), rabbit polyclonal anti phospho-SRC (Cat# sc-166860, [RRID:AB_10611497](#)), mouse monoclonal anti MEF2D(H11) (Cat# sc-271153), or mouse monoclonal anti GAPDH (Cat# sc-365062, [RRID:AB_10847862](#)) from Santa Cruz Biotechnology (Santa Cruz, CA, USA); rabbit polyclonal anti SK1 (Cat# SP1621, [RRID:AB_2195828](#)) or rabbit polyclonal anti SK2 (Cat# SP4621, [RRID:AB_2619719](#)) from ECM Biosciences (Aurora, CO, USA); rabbit polyclonal anti S1P₁ (Cat# ab11424, [RRID:AB_298029](#)), rabbit polyclonal anti S1P₃ (Cat# ab126622, [RRID:AB_11140549](#)) from Abcam (Cambridge, UK); rabbit polyclonal anti S1P₂ (Cat# 21180-1-AP, [RRID:AB_10694573](#)) from Proteintech (Rosemont, IL, USA); rabbit polyclonal anti SPL (Cat# PA1-12722, [RRID:AB_2285994](#)) from Thermo Fisher Scientific Inc. (Rockford, IL, USA); mouse monoclonal anti vinculin (Cat #V9131, [RRID:AB_477629](#)) or rabbit polyclonal anti Spns2 (Cat# SAB2104271, [RRID:AB_10696636](#)) from Sigma-Aldrich.

2.4 | Cell transfection

Lipofectamine RNAiMAX (Invitrogen, Carlsbad, CA) was used for cell transfection according to the manufacturer's instructions as previously described.^{34,35} Lipofectamine RNAiMAX was incubated with siRNAs (siRNA universal negative control SIC001; siS1P₁ SASI_HS_0024; siS1P₂ SASI_HS01_0008; siS1P₃ SASI_HS01_0001, Sigma Aldrich [RRID:SCR_008988](#); siERK5, M0035130200 Dharmacon, Thermo Fisher Scientific Inc.) in DMEM:F12 (1:1) without serum and antibiotics at room temperature for 20 min and then added to cells to a final concentration of 50 nmol/L, in DMEM:F12 (1:1) containing serum. After 56 h, cells were serum-starved overnight and were used for experiments 72 h after the beginning of transfection. The efficacy of target down-regulation was evaluated with the use of quantitative real-time polymerase chain reaction or Western blot analysis. The pcMV5-MEK5DD-HA (a constitutively active form of MEK5) was generously provided by Jiing-Dwan Lee (Scripps Institute, La Jolla, CA, USA). HESC were plated (3×10^4 cells/well) and transfected after 24 h with a total amount of 2 µg of plasmid DNA using Lipofectamin2000 (Invitrogen, Thermo Fisher Scientific), following manufacturer's instructions. Cells were used for experiments 24 h after the beginning of transfection.

2.5 | Quantitative real-time PCR (qPCR)

Total RNA was extracted from the cells using TRI-reagent (Sigma-Aldrich) according to the manufacturer's instructions, and reverse transcribed with the high-capacity cDNA

reverse transcription kit (Applied Biosystems) as previously described.^{36,37} The quantification of target mRNA expression through qPCR was performed using TaqMan gene expression assays (SK1 Hs00184211_m1, SK2 Hs01016543_g1, CIB1 Hs01089679_m1, SPL Hs00393705_m1, SPP1 Hs04189357_m1, SPP2 Hs00544786_m1, S1P₁ Hs01922614_s1, S1P₂ Hs_01003373_M1; S1P₃ Hs00245464_s1, S1P₄ Hs02330084_s1, S1P₅ Hs00928195_s1; Spns2 Hs01390449_g1; IL1 β Hs01555410_m1; IL-6 Hs00174131_m1) (Thermo Fisher Scientific) or using GoTaq qPCR Master Mix (Promega Corporation). The primers used were the following: ERK5 mRNA fw 5'-TGCCCCACCAAAGAAAGATG-3', rev 5'-AAGAC TTGAGCAGGGCAGCTT-3'; 18S rRNA fw 5'-CGGTA CCACATCCAAGGAA-3', rev 5'-GCTGGAATTACCGC GGCT-3'. qPCR was performed using CFX96 Touch Real-Time PCR Detection System (Bio-Rad). Target sequences were simultaneously amplified together with the housekeeping gene β -actin or 18S rRNA. Relative quantification of mRNA expression was performed by means of the $2^{-\Delta\text{Ct}}$ method³⁸ for tissue samples or the $2^{-\Delta\Delta\text{Ct}}$ method³⁹ for cellular samples.

2.6 | Confocal microscopy

Cells were seeded on a glass coverslip and, at the end of treatment, incubated with the probe chloromethyl derivative of 2',7'-dichlorodihydrofluorescein diacetate (CM-H₂DCFDA; Thermo Fisher Scientific) 5 μ M for 20 min, as an indicator for reactive oxygen species (ROS) in cells. Fluorescence was assessed with confocal microscopy (Leica SP8) and quantified using the ImageJ software (RRID:SCR_003070, National Institutes of Health, USA).

2.7 | Flow cytometry

After treatment, cells were incubated with CM-H₂DCFDA 1 μ M for 20 min. Cells were then detached with Trypsin-EDTA solution (Sigma-Aldrich) and cell fluorescence was measured with a FACSCanto flow-cytometer (Becton-Dickinson, Franklin Lakes, NJ, USA).

2.8 | Statistical analysis

Statistical analysis and graphical representations of the data were performed using the GraphPad Prism 5 software (RRID:SCR_002798). P values were calculated using Student's *t* test (two groups), one-way analysis of variance ANOVA (more than two groups) followed by Bonferroni post hoc test or two-way ANOVA followed by

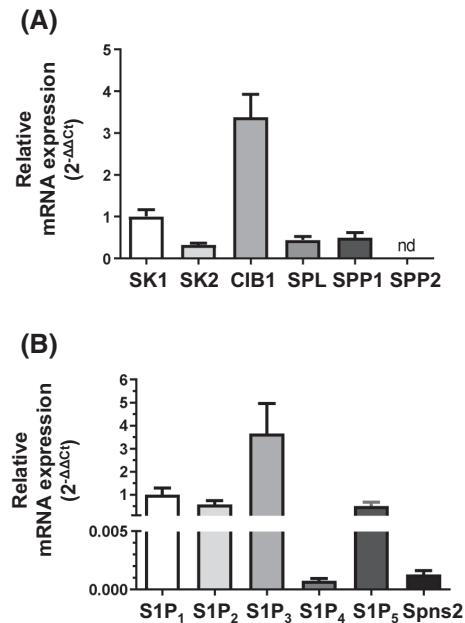


FIGURE 1 S1P metabolism enzyme, transporter, and S1PR expression levels in HESC. HESC were seeded in 60 mm dishes at 70% confluence. qPCR analysis was performed using TaqMan gene expression assay probes specific for human SK1, SK2, CIB1, SPL, SPP1, and SPP2 (A) and S1P₁₋₅ and Spns2 (B). Results, analyzed with the $2^{-\Delta\Delta\text{Ct}}$ method, were normalized to β -actin housekeeping gene and expressed as fold changes over a reference gene, SK1 (A), and S1P₁ (B). nd, not detected.

Bonferroni post hoc test. $p < .05$ was considered statistically significant.

3 | RESULTS

3.1 | S1P stimulation increases ROS production in human endometrial stromal cells

Although S1P metabolism and signaling are dysregulated in endometriosis,^{17,18} the molecular mechanisms implicated in the action of this sphingolipid in the pathogenesis of the disease have not been profoundly investigated so far. To deepen this issue, we first investigated whether human endometrial stromal cells (HESC) express the enzymes involved in S1P metabolism and the S1PR (Figures 1 and S1). qPCR analysis showed that both isoforms of sphingosine kinase (SK), SK1 and SK2, and the enzymes involved in S1P catabolism, S1P lyase (SPL) and S1P phosphatase (SPP)1, but not SPP2, were expressed in HESC (Figure 1A). In addition, HESC expressed the SK1-activating protein CIB1 (Figure 1A). At the mRNA level, the S1P transporter Spns2 and all S1PR were expressed, being S1P₃ the most expressed receptor (Figure 1B). The

expression of SK1, SK2, SPL, Spns2 as well as S1P₁/S1P₂/S1P₃ was confirmed at the protein level by Western blot analysis (Figure S1).

Given the key role of ROS in the progression of inflammatory disorders, we investigated whether S1P was able to induce ROS formation in HESC. Intracellular ROS levels were detected by confocal immunofluorescence analysis performed using CM-H₂DCFDA. We found that the treatment with 100 nM S1P for 10 min potently increased ROS formation in HESC (Figure 2A). In agreement, cytofluorimetric ROS quantification highlighted a significant increase of about 40% following 10 min treatment with 100 nM S1P (Figure 2B).

3.2 | S1P activates ERK5 through S1P₁ and S1P₃ receptor engagement and downstream activation of SFK and MEK5

We then examined whether, in HESC, S1P was capable of activating ERK5, a pivotal MAPK involved in ROS modulation,⁴⁰ expressed in endometrial tissues and endometriotic lesions as determined by qPCR (Figure 3A). To this end, HESC were treated with 100 nM S1P for different time intervals (from 5 to 60 min) before being lysed and subjected to Western blot analysis. ERK5 activation was then evaluated on the basis of the presence of a band-shift due to decreased ERK5 electrophoretic mobility following extensive phosphorylation as the consequence of MEK5-dependent phosphorylation in the conserved threonine-glutamic acid-tyrosine (TEY) motif of the catalytic domain and MEK5-independent phosphorylation at the C-terminus.^{27,41} As depicted in Figure 3B, S1P transiently activated ERK5 with a maximal overall phosphorylation at 10 min of treatment. In particular, treatment with the sphingolipid determined MEK5-dependent phosphorylation, as witnessed by increased phosphorylation of the TEY motif. ERK5 activation was confirmed by the increased p90RSK phosphorylation and MEF2D expression that are ERK5-regulated downstream targets.^{42,43} Dose-dependence studies showed that ERK5 activation was induced by S1P at all the tested concentrations (10–1000 nM) being maximal starting from 100 nM (Figure 3C). Accordingly, S1P induced a dose-dependent increase of ERK5 phosphorylation on TEY motif, of p90RSK phosphorylation and of MEF2D expression.

We next examined the possible S1PR involved in S1P-induced ERK5 activation. For this purpose, S1P₁, S1P₂, and S1P₃ were efficiently knocked-down by specific siRNA (Figure 4A). Moreover, to further verify that S1PR silencing affected their functional activity, the activation of known S1PR downstream targets^{37,44} has been analyzed. In particular, while S1P₁ and S1P₃ silencing significantly

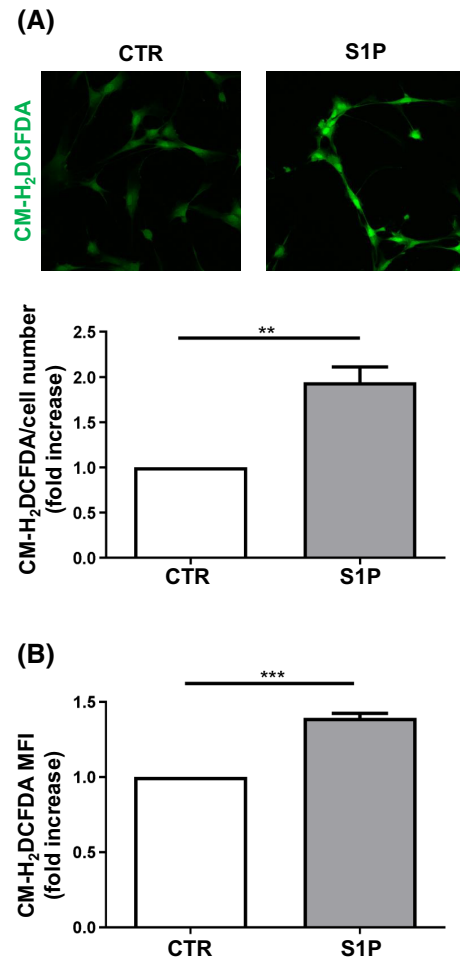
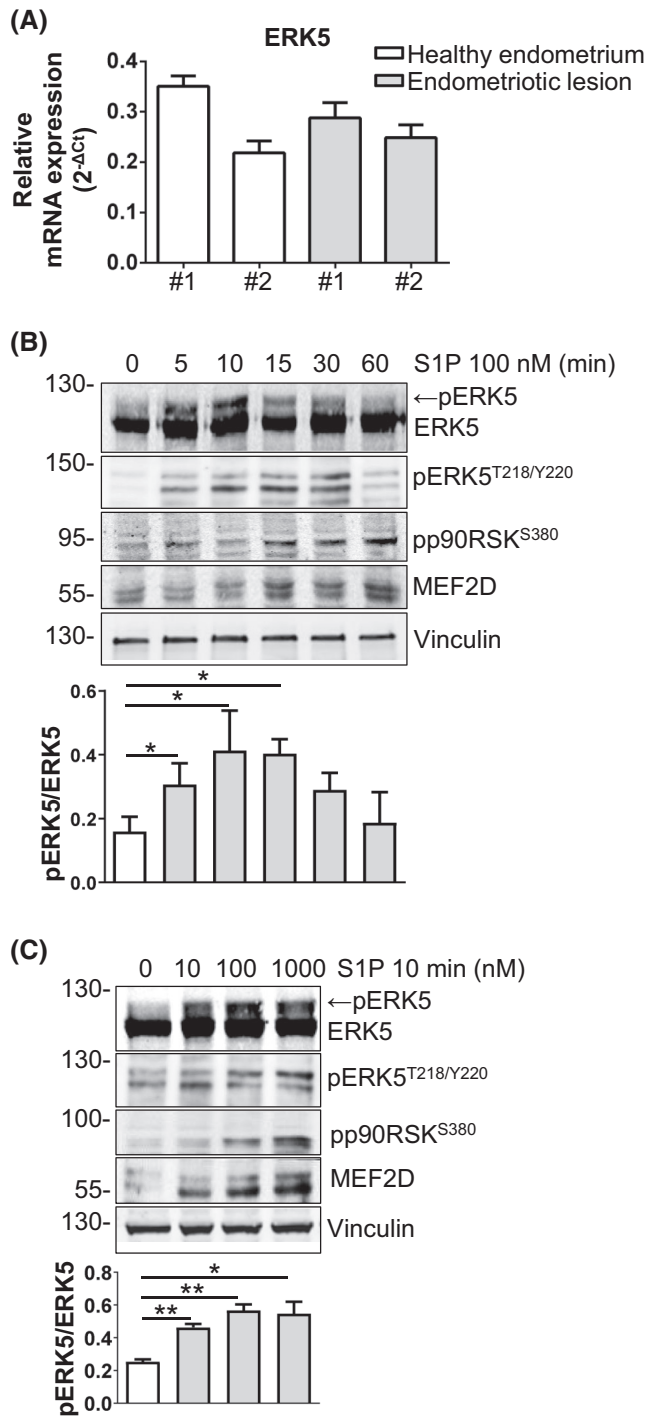


FIGURE 2 S1P stimulates ROS production. (A) HESC seeded on microscope slides were serum-starved for 18 h before being stimulated with 100 nM S1P for 10 min. Upper panel: images were obtained by confocal microscopy analysis using CM-H₂DCFDA to stain ROS (images are representative of three independent experiments). Lower panel: quantification of the intensity of CM-H₂DCFDA fluorescence normalized to cell number. Data are mean \pm SEM of four fields quantified in three independent experiments. S1P increases ROS formation in a statistically significant manner by *t*-test $**p < .01$. (B) HESC were serum-starved for 18 h before being stimulated with 100 nM S1P for 10 min. ROS were quantified by cytofluorimetric analysis using CM-H₂DCFDA. Results are reported as mean \pm SEM of eight independent experiments, fold change over control set as 1. S1P increases ROS formation in a statistically significant manner by *t*-test ($***p < .001$). MFI, mean fluorescence intensity.

reduced S1P-induced ERK1/2 phosphorylation, that of S1P₂ inhibited the S1P-induced ERM activation in HESC (Figure S2). Notably, as shown in Figure 4B, siRNA directed against S1P₁ and S1P₃ significantly reduced the enhancement of ERK5 activation elicited by S1P. Conversely, the down-regulation of S1P₂ did not alter the S1P-induced effect (Figure 4B). To confirm the role of S1P₁ and S1P₃ in S1P-induced ERK5 activation, pharmacological inhibition



of both S1PR was performed using the S1P_{1/3} antagonist VPC23019. As shown in Figure 4C, the activation of ERK5, induced by S1P, was prevented by preincubation with VPC23019. All together, these data support the view that S1P activates ERK5 through S1P₁ and S1P₃ engagement.

To gain insight into the implicated molecular mechanism, we considered pathways that are known to be activated by G-protein-coupled receptors and, in turn, are involved in ERK5 activation such as SRC-family kinases (SFK), MEK5, and ERK1/2.²⁸ As reported in Figure 5A,

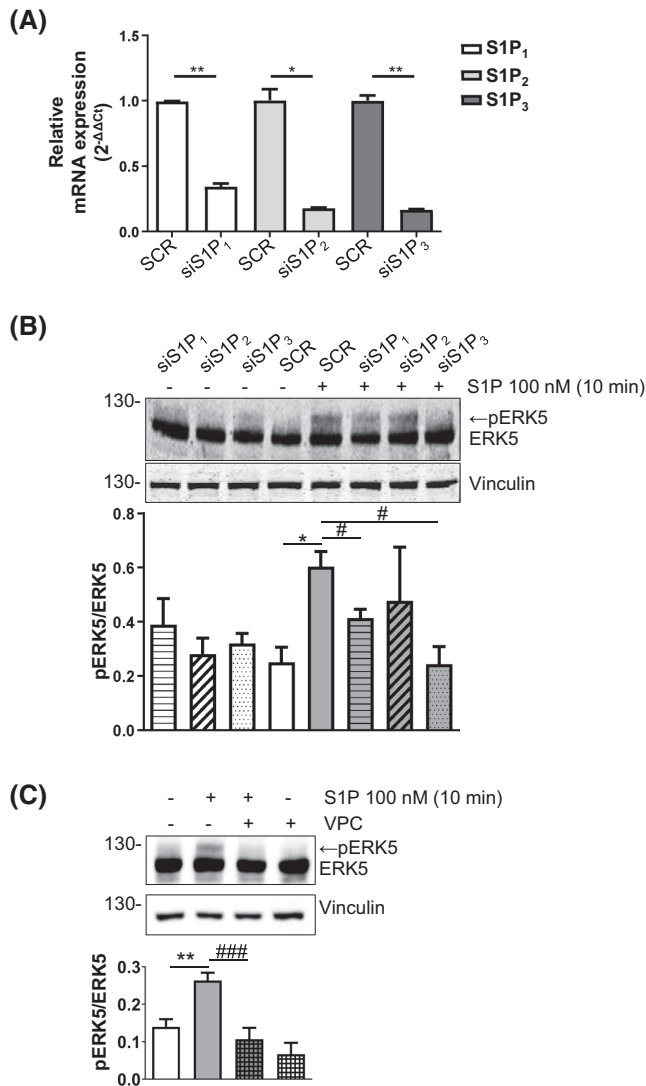
FIGURE 3 S1P activates ERK5. (A) Quantitative mRNA analysis was performed by qPCR in total RNA extracted from healthy endometrium ($n=2$) and endometriotic lesions ($n=2$). Results, analyzed with the $2^{-\Delta\Delta Ct}$ method, were normalized to 18S housekeeping gene. HESC were serum-starved for 18 h and then treated for different time intervals (5–60 min) with 100 nM S1P (B) or with S1P at the indicated concentrations (10–1000 nM) for 10 min (C). Western blot analysis was performed using anti-ERK5, -pERK5^{T218/Y220}, -pp90RSK^{S380}, -MEF2D. Migration of molecular weight markers is indicated on the left (kDa). Upper panels: blot representative of at least three independent experiments with analogous results is shown. Lower panels: densitometric analysis of at least three independent experiments. Data are fold change over control (set as 1) of the mean \pm SD of the ratio between the slower migrating upper ERK5 band (indicated by the arrow) and the lower ERK5 band normalized to vinculin. One-way ANOVA followed by Bonferroni's post hoc test (* $p < .05$ ** $p < .01$, treated vs. control).

10 min stimulation with 100 nM S1P was responsible for MEK5, SRC, and ERK1/2 activation in HESC. Subsequently, HESC were pretreated with the MEK5 inhibitor BIX02189 (5 μ M), the SFK inhibitor PP2 (10 μ M), or the ERK1/2 inhibitor SCH772984 (1 μ M). As shown in Figure 5B the band-shift of ERK5, induced by S1P, was prevented by preincubation with BIX02189 or PP2, but not by SCH772984, demonstrating that the bioactive sphingolipid activates ERK5 through SFK and MEK5.

3.3 | ERK5 is involved in S1P-dependent intracellular ROS formation

We next examined the potential role of S1P-dependent activation of ERK5 in the induction of intracellular ROS formation. For this purpose, HESC were treated with 5 μ M XMD8-92 or 5 μ M JWG-071, pharmacological inhibitors of ERK5, before being challenged with 100 nM S1P for 10 min. Confocal fluorescence analysis (Figure 6A) as well as cytofluorimetric quantification (Figure 6B) clearly demonstrated that the enhanced formation of ROS induced by S1P was completely reversed by ERK5 inhibition. To further confirm the role of ERK5 in the modulation of ROS levels evoked by S1P, ERK5 was knocked-down by RNA interference. The specific siRNA treatment efficaciously reduced basal expression levels of ERK5 (Figure S3), and significantly reduced S1P-induced intracellular ROS increase measured by cytofluorimetric analysis (Figure 6C). Of note, activation of ERK5 by the expression of a constitutively active form of MEK5 (MEK5DD) significantly increased intracellular ROS, confirming the role of MEK5-dependent phosphorylation of ERK5 in the modulation of ROS levels in HESC (Figure S4).

In order to demonstrate whether S1P-induced ROS production is a S1PR-mediated event, we down-regulated by RNA interference S1P₁ and S1P₃, previously shown to be



involved in the activation of ERK5 elicited by the sphingolipid (Figure 4B,C). Cytofluorimetric analysis demonstrated that S1P-induced intracellular ROS increase was significantly reduced by siRNA directed against S1P₁ or S1P₃ (Figure 6D) or pharmacological blockade of S1P_{1/3} using VPC23019 (Figure 6E).

3.4 | S1P induces IL-1β and IL-6 expression via ERK5 activation and ROS formation

Then, we examined whether S1P was able to induce a pro-inflammatory response in endometrial cells by increasing the synthesis of cytokines. To this end, the mRNA expression of IL-1β and IL-6 was examined in HESC treated with 100 nM S1P for 6 h. qPCR analysis demonstrated that the sphingolipid increased the expression of the above pro-inflammatory cytokines (Figure 7A). This effect was impaired by S1P_{1/3} antagonism, using VPC23019 (Figure 7A), pointing to the involvement of these receptors in

FIGURE 4 S1P activates ERK5 via S1P₁ and S1P₃. (A) Relative quantitative mRNA analysis was performed by qPCR in HESC transfected with nonspecific siRNA (SCR) or with siRNA specific for S1P₁ or S1P₂ or S1P₃; the content of housekeeping gene β-Actin was analyzed in parallel. Results are expressed as fold changes according to the 2^{-ΔΔCt} method, utilizing as calibrator each receptor subtype in cells transfected with SCR siRNA. Data are mean ± SEM of three independent experiments performed in triplicate. The effect of S1P₁-S1P₂ and S1P₃-siRNA transfection is statistically significant by *t*-test **p* < .05, ***p* < .01. (B) HESC transfected with SCR-, S1P₁-S1P₂- and S1P₃-siRNA were serum-starved prior to be stimulated with 100 nM S1P for 10 min. ERK5 activation was measured in total cell lysate by Western blotting using anti-ERK5 antibody. Migration of molecular weight markers is indicated on the left (kDa). Data are fold change over control (set as 1) of the mean ± SD of the ratio between the slower migrating upper ERK5 band (indicated by the arrow) and the lower ERK5 band normalized to vinculin. A blot representative of three independent experiments is shown. S1P activates ERK5 in a statistically significant manner (**p* < .05). The effect of S1P₁- or S1P₃-downregulation on S1P-induced ERK5 activation is statistically significant by two-way ANOVA followed by Bonferroni's post hoc test (#*p* < .05). (C) Serum-starved HESC were pretreated with the pharmacological inhibitor of S1P_{1/3} VPC23019 (VPC, 10 μM) for 1 h before being challenged with 100 nM S1P for 10 min. ERK5 activation was measured in total cell lysate by Western blotting using anti-ERK5 antibody. Migration of molecular weight markers is indicated on the left (kDa). A blot representative of three independent experiments with analogous results is shown. The histogram represents the densitometric analysis of three independent experiments; data are the mean ± SD of the ratio between ERK5 up-shifted band/ERK5 normalized to vinculin, fold change over control (set as 1). S1P activates ERK5 in a statistically significant manner (***p* < .01). The effect of S1P_{1/3} blockade by VPC23019 on S1P-dependent ERK5 activation is statistically significant by two-way ANOVA followed by Bonferroni's post hoc test (###*p* < .001).

S1P-elicited increase of IL-1β and IL-6. In order to establish the potential role of S1P-dependent ERK5 activation in the proinflammatory action of the sphingolipid, HESC were pretreated for 1 h with the ERK5 inhibitor XMD8-92 (5 μM) or transfected with specific siRNA for ERK5 before being challenged with 100 nM S1P for 6 h. qPCR analysis demonstrated that both pharmacological (Figure 7B) and genetic (Figure 7C) inhibition of ERK5 significantly diminished the S1P-dependent increase of IL-1β and IL-6. The same effects were elicited upon pretreatment with the ROS scavenger NAC (5 mM) (Figure 7D), thus providing evidence of the involvement of ROS in the S1P-induced production of the above proinflammatory cytokines. Interestingly, pharmacological inhibition of ERK5 strongly reduced the basal expression levels of the analyzed proinflammatory cytokines (Figure 7B), in line with the data shown in Figure S4 and with previous reports^{40,45} and further supporting a crucial role for this MAPK in the regulation of the inflammatory response in the endometrium.

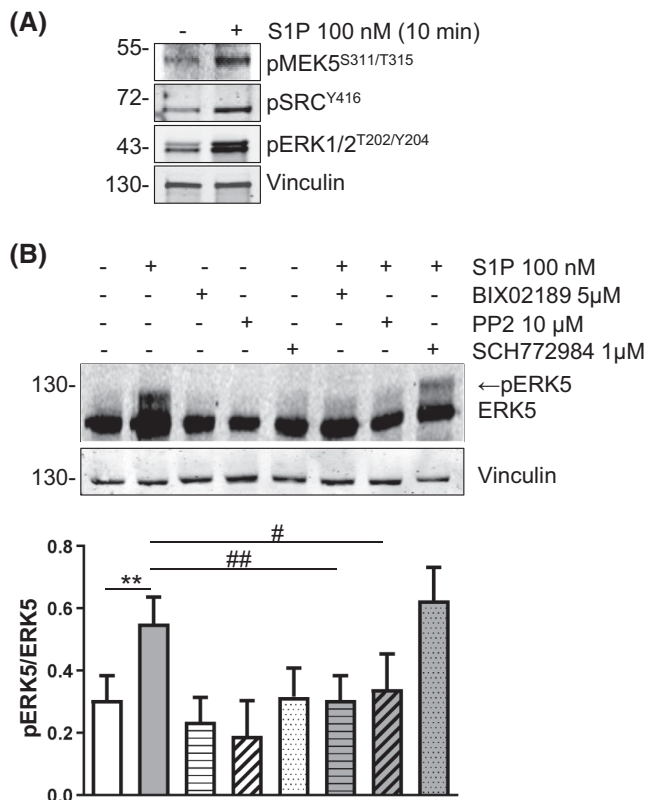


FIGURE 5 S1P activates ERK5 via SFK and MEK5. (A) HESC were serum-starved for 18 h and then treated for 10 min with 100 nM S1P. Western blot analysis was performed using antibodies for the phosphorylated forms of MEK5, SRC, and ERK1/2 in cell lysates. Migration of molecular weight markers is indicated on the left (kDa). A blot representative of two independent experiments with analogous results is shown. (B) Serum-starved HESC were pretreated with 5 μ M BIX02189, selective inhibitor of MEK5, or 10 μ M PP2, specific inhibitor of SFK, or 1 μ M SCH772984, specific inhibitor of ERK1/2, for 1 h before being challenged with 100 nM S1P for 10 min. ERK5 activation was measured in total cell lysate by Western blotting using anti-ERK5 antibody. Migration of molecular weight markers is indicated on the left (kDa). A blot representative of three independent experiments with analogous results is shown. The histogram represents the densitometric analysis of three independent experiments; data are the mean \pm SD of the ratio between ERK5 up-shifted band/ERK5 normalized to vinculin, fold change over control (set as 1). S1P activates ERK5 in a statistically significant manner (** $p < .01$). The effect of SFK inhibition by PP2 or MEK5 inhibition by BIX02189 on S1P-dependent ERK5 activation is statistically significant by two-way ANOVA followed by Bonferroni's post hoc test ($^{\#}p < .05$, $^{\#\#}p < .01$).

4 | DISCUSSION

Inflammation is one of the key mechanisms in the pathophysiology of endometriosis, involved in lesion formation, fibrosis, and infertility.^{3,4,46–48} The investigation of the molecular mechanisms involved in the pathogenesis of the inflammatory process could open new perspectives

to identify novel therapeutic strategies for endometriosis. The findings presented here show that the bioactive sphingolipid S1P is responsible for the activation of ERK5, and the identified S1P/ERK5 axis emerged to be crucial in supporting a ROS-mediated proinflammatory effect in endometrial cells.

Several lines of evidence support the role of oxidative stress in the development and progression of endometriosis by causing a general inflammatory response in the peritoneal cavity.^{49,50} Along this line, S1P has been largely involved in both acute and chronic inflammation, by regulating immune cell recruitment.⁵¹ In human intraperitoneal macrophages, S1P provoked a shift toward an M2-dominant condition and an increased expression of IL-6 and COX2, thus determining an extension of the endometriotic lesion size.¹⁹ In the present study, we demonstrated that S1P stimulation increases ROS production in endometrial cells, thus pointing to the existence of a link between S1P and oxidative stress in endometriosis. This is in agreement with a previous study performed in human pulmonary alveolar epithelial cells showing that S1P increased the inflammatory response through a NADPH oxidase/ROS-dependent NF- κ B activation mechanism.⁵² Moreover, in bone marrow-derived macrophages, S1P/S1P₂ signaling axis was responsible for ROS production and NLRP3 inflammasome activation.⁵³ Thus, our data, in keeping with other reports,^{52–54} support the evidence that S1P is a lipid engaging a redox-based signaling. Here, the identification of S1P_{1/3} as responsible for ROS generation in endometrial cells in response to S1P treatment further highlights that the signaling mediated by S1PR is cell-specific.

Many studies have emphasized the importance of MAPKs in the development and progression of endometriosis.^{55–57} Additionally, both in vitro and in vivo investigations have shown that activation of the MEK5/ERK5 pathway is involved in oxidative stress-elicited effects.^{40,58–60} We here reported for the first time that S1P induces ERK5 activation in endometrial cells and that both pharmacological and genetic inhibition of ERK5 reverted the S1P-dependent ROS production and proinflammatory cytokine expression. Very little literature evidence is available on the ability of S1P to activate ERK5. The sphingolipid has been reported to activate this MAPK kinase in mouse embryonic fibroblasts in PTX-independent manner⁶¹ and in HEK293 overexpressing ERK5.⁶² Interestingly, in the present study, ERK5 was found to be expressed in endometriotic lesions.

Another interesting finding illustrated here is the identification of the molecular mechanism implicated in S1P-induced ERK5 activation. Indeed, we demonstrated that S1P₁ and S1P₃ mediate S1P-dependent increase in ERK5 activation.

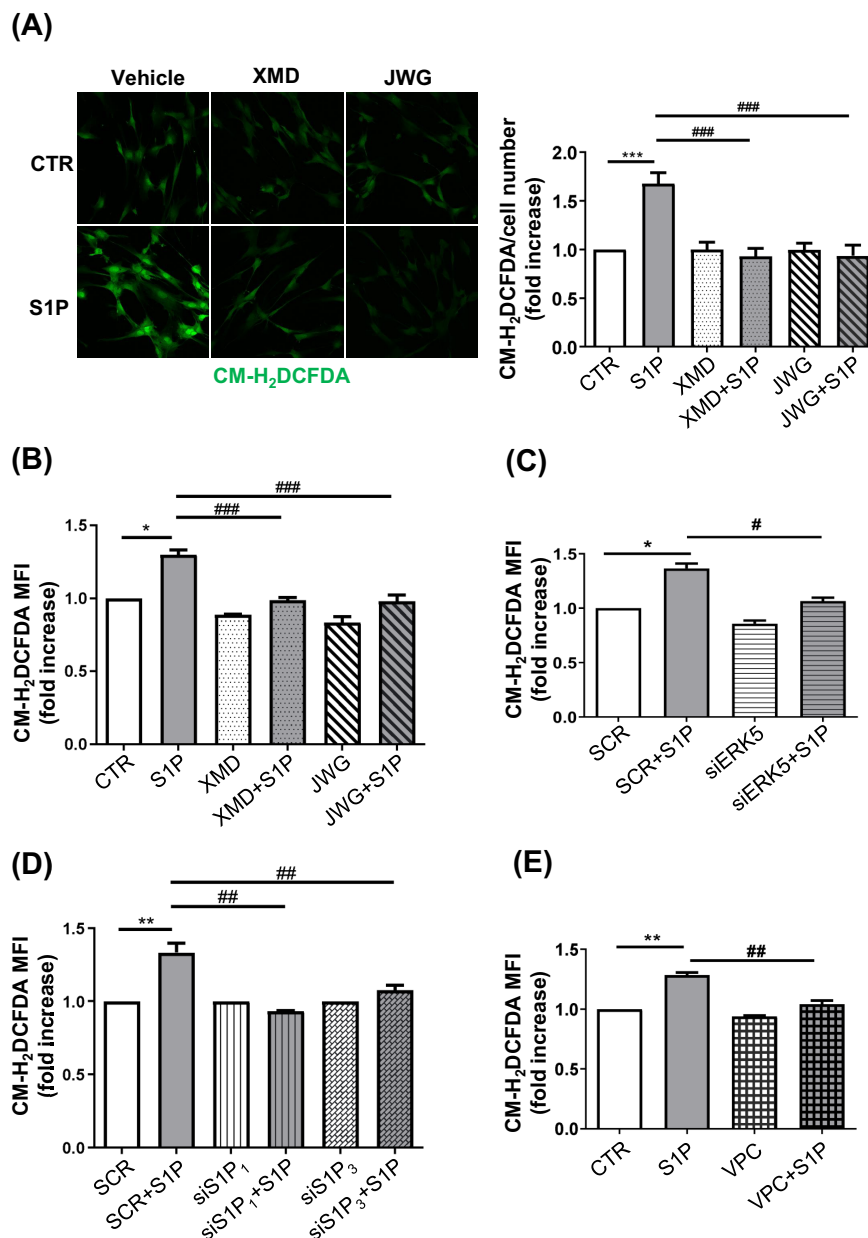


FIGURE 6 S1P-induced ROS production relies on ERK5 activation. (A) HESC seeded on microscope slides were serum-starved for 18 h and pretreated or not with the ERK5 inhibitors XMD8-92 (XMD) 5 μ M or JWG-071 (JWG) 5 μ M for 1 h before being stimulated with 100 nM S1P for 10 min. Left: images were obtained by confocal microscopy analysis using CM-H₂DCFDA to stain ROS (images are representative of three independent experiments). Right: quantification of the intensity of CM-H₂DCFDA fluorescence normalized to cell number. Data are mean \pm SEM of four fields quantified in three independent experiments. S1P increases ROS formation in a statistically significant manner ($***p < .001$). The effect of ERK5 inhibition by XMD8-92 or JWG-071 on S1P-induced ROS formation is statistically significant by two-way ANOVA followed by Bonferroni's post hoc test ($###p < .001$). HESC were serum-starved for 18 h and pretreated or not with the ERK5 inhibitors XMD8-92 (XMD) 5 μ M or JWG-071 (JWG) 5 μ M (B) or the pharmacological inhibitor of S1P_{1/3} VPC23019 (VPC, 10 μ M) (E) for 1 h before being stimulated with 100 nM S1P for 10 min. HESC, transfected with SCR- or ERK5-siRNA (C) or with SCR-, S1P₁- and S1P₃-siRNA (D), were serum-starved prior to be stimulated with 100 nM S1P for 10 min. ROS were quantified by cytofluorimetric analysis using CM-H₂DCFDA. Results are reported as mean \pm SEM of an experiment representative of four, performed in duplicate, fold change over control set as 1. S1P increases ROS formation in a statistically significant manner ($*p < .05$; $**p < .01$). The effect of ERK5 pharmacological inhibition by XMD8-92 or JWG-071 (B) or ERK5 silencing (C) or S1P₁- or S1P₃-silencing (D) or S1P_{1/3} blockade by VPC23019 (E) on S1P-induced ROS formation is statistically significant by two-way ANOVA followed by Bonferroni's post hoc test ($^{\#}p < .05$; $^{\#\#}p < .01$; $^{\#\#\#}p < .001$). MFI, mean fluorescence intensity.

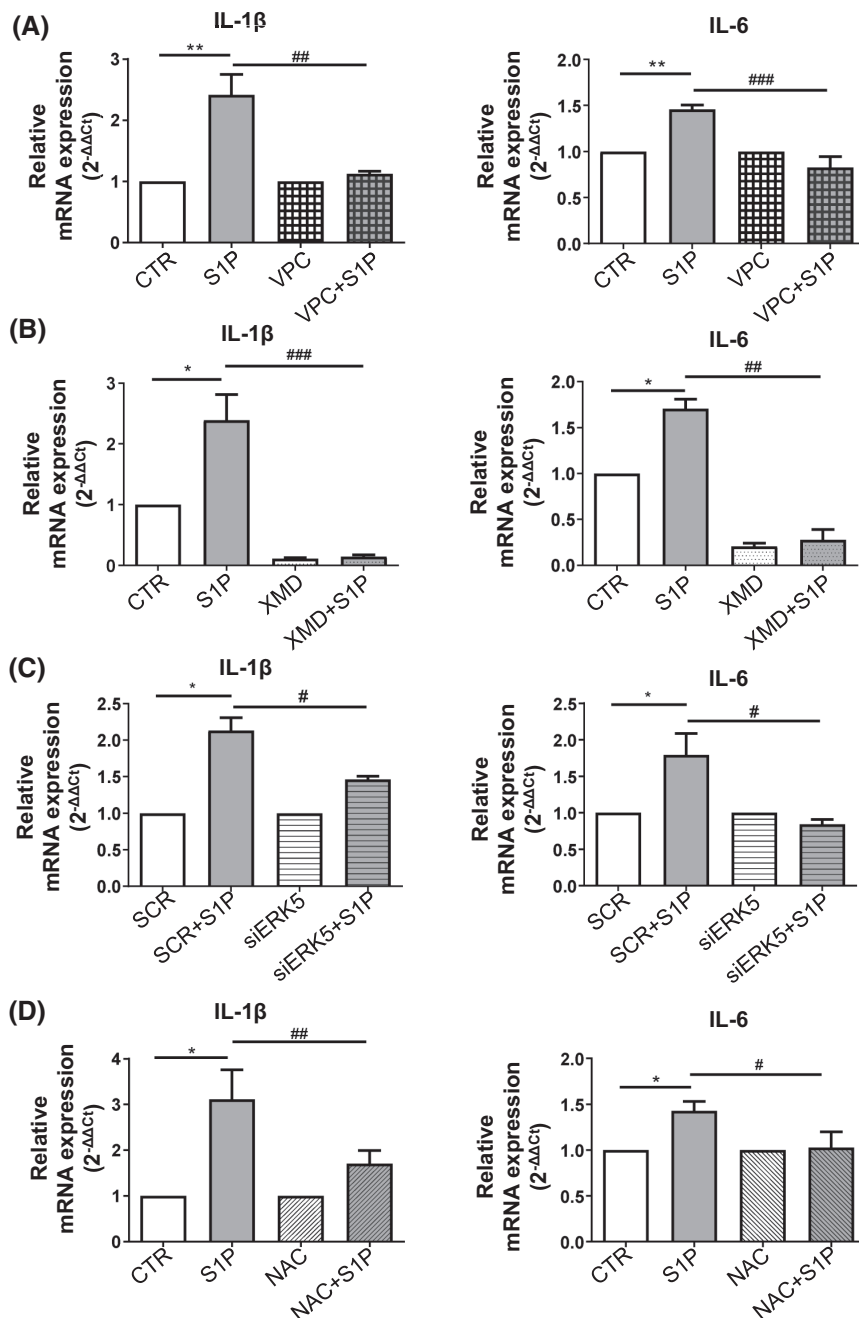


FIGURE 7 S1P induces IL-1 β and IL-6 expression via ERK5 activation and ROS formation. HESC were serum-starved for 18 h and pretreated or not with the S1P_{1/3} antagonist VPC23019 (VPC, 10 μ M) (A) or the ERK5 inhibitor XMD8-92 (XMD, 5 μ M) (B) or the ROS scavenger NAC (5 mM) (D) for 1 h before being stimulated with 100 nM S1P for 6 h. HESC transfected with SCR- or ERK5-siRNA (C) were serum-starved prior to be stimulated with 100 nM S1P for 6 h. Quantitative analysis of IL-1 β and IL-6 mRNA was performed by real-time PCR. Results are expressed as fold changes according to the 2^{-ΔΔCt} method, using individual cytokines of the unchallenged specimen as calibrator. S1P increases IL-1 β and IL-6 expression in a statistically significant manner (* p < .05; ** p < .01). The effect of S1P_{1/3} blockade by VPC23019 (A) or ERK5 inhibition by XMD8-92 (B) or ERK5-downregulation by specific siRNA (C) or ROS scavenging by NAC (D) on S1P-induced cytokine mRNA levels was statistically significant by two-way ANOVA followed by Bonferroni's post hoc test (# p < .05, ## p < .01, ### p < .001).

Although it is known that intracellular S1P can evoke inflammatory responses mainly by NF- κ B activation, recent studies support the involvement of S1PR and thus of an extracellular pool of S1P in this process. The involvement of S1P_{1/3} in the induction of IL-6, COX-2 as well as prostacyclin was also demonstrated in endothelial cells where S1P cooperates with LPS in leukocyte adhesion.⁶³ Moreover, in different cancer cell types, S1P₁ induces persistent STAT3 activation and IL-6 expression.⁶⁴ S1P₁ but also S1P₂ was instead found to mediate NF- κ B activation and IL-6 expression in melanoma cells,⁶⁵ while S1P₂ was also implicated in the induction of IL-6 expression in endometriotic stromal cells derived from endometrioma.²⁰ In this work, the involvement of S1P₂ in ERK5 activation

was excluded since when the receptor was silenced by RNA interference the effect of the sphingolipid was not significantly altered. Crucially, it was previously shown that a deep remodeling of S1PR occurs at the level of endometriotic lesions when compared with healthy endometrium controls.^{17,18}

S1P has been previously reported to induce SRC activation, in turn responsible for NADPH oxidase activation and H₂O₂ production in NIH/3T3 fibroblasts as well as COX-2 expression and PGE₂/IL-6 secretion in human tracheal smooth muscle cells.⁶⁶ Moreover, SRC has been extensively demonstrated to be an upstream activator of the MEK5/ERK5 module in many cell types.²⁴ In line with the above findings, we show here that the bioactive

sphingolipid activates ERK5 through SFK. In this respect, it is worth noting that despite ERK5 inhibition almost completely impaired S1P-induced ROS production, we may not exclude that activation of the SFK/MEK5/ERK5 signaling is ROS-dependent.^{40,67,68} On the other hand, our data indicate that S1P-induced ERK5 activation is mediated by MEK5, in line with the well-established notion that ERK5 activation is classically operated by its upstream MAPKK, MEK5, that has ERK5 as its only known substrate.⁶⁹ To our knowledge, this is the first evidence of MEK5 activation by the bioactive sphingolipid. At variance with what is reported in certain cellular models,^{32,70} ERK1/2 does not seem to be involved in S1P-mediated ERK5 activation in endometrial cells.

Proinflammatory mediators are involved in the onset and worsening of endometriosis.⁷¹ In the present work, we found that S1P increases the expression of IL-6 and IL-1 β in endometrial cells and that ERK5 inhibition abrogated this increase, thus supporting the hypothesis of the involvement of ERK5 in S1P-mediated regulation of the inflammatory response in the endometrium. These findings are in keeping with the fact that serum IL-6 has been identified in high concentrations in endometriosis⁷² and that the level of its expression has been linked to the disease severity.⁷³ Moreover, the expression of IL-1 β , which has been associated with the risk of endometriosis,⁷⁴ appears to depend on the stage of the disease and stimulates the upregulation of biomolecules that induce pain.⁷⁵

In conclusion, our findings support the view that the S1P signaling via ERK5 activation supports a proinflammatory response in the endometrium and establish the rationale for the exploitation of S1P/ERK5 targeting as an innovative therapeutic approach in endometriosis.

AUTHOR CONTRIBUTIONS

CB, CD ER, and IT conceived and designed the research. AM, CB, IS, IT, and MP performed the research and acquired the data. FP and SV collected biological samples; FCa performed the histological characterization of the biological samples. CB, CD, ER, FCe, IS, and IT analyzed and interpreted the data. CB, CD, ER, IS, and IT wrote the manuscript. FP and PB revised the paper.

ACKNOWLEDGMENTS

We took advantage of the newly established Molecular Medicine Facility of the Department of Experimental and Clinical Biomedical Sciences “Mario Serio” at the University of Florence. The Facility was supported by a grant of the Italian Ministry of Education University and Research (MIUR) after the Department was awarded as one of the 180 Departments of Excellence in Italy.

FUNDING INFORMATION

The work was supported by Fondi di Ateneo (ex 60%) to CB, CD, ER, FCe, FP, and PB, by MIUR, Progetto Medicina di Genere to CD, by Fondazione Careggi, Project on Woman's Health, by Fondazione Cassa di Risparmio di Firenze to FP, by Associazione Italiana per la Ricerca sul Cancro (AIRC) to ER and by Università degli Studi di Firenze (“Progetto Competitivo di Ateneo per Ricercatori” funded by MUR and Next Generation EU) to ER.

DISCLOSURES

The authors declared that they have no conflict of interest to this work.

DATA AVAILABILITY STATEMENT

All data generated or analyzed during this study are included in this published article. The analyzed datasets and materials used in the current study are available from the corresponding authors on reasonable request.

ORCID

Isabelle Seidita  <https://orcid.org/0000-0002-7777-1124>

Ignazia Tusa  <https://orcid.org/0000-0002-9198-2630>

Matteo Prisinzano  <https://orcid.org/0000-0002-0238-7101>

Alessio Menconi  <https://orcid.org/0000-0001-8264-7462>

Francesca Cencetti  <https://orcid.org/0000-0003-4351-2965>

Silvia Vannuccini  <https://orcid.org/0000-0001-5790-587X>

Francesca Castiglione  <https://orcid.org/0000-0003-1696-5651>

Paola Bruni  <https://orcid.org/0000-0002-1151-3413>

Felice Petraglia  <https://orcid.org/0000-0002-8851-625X>

Caterina Bernacchioni  <https://orcid.org/0000-0002-1023-0067>

Elisabetta Rovida  <https://orcid.org/0000-0002-5949-3239>

Chiara Donati  <https://orcid.org/0000-0003-2224-4199>

REFERENCES

- Zondervan KT, Becker CM, Missmer SA. Endometriosis. *N Engl J Med*. 2020;382:1244-1256.
- Zondervan KT, Becker CM, Koga K, Missmer SA, Taylor RN, Viganò P. Endometriosis. *Nat Rev Dis Primers*. 2018;4:9.
- Bulun SE, Yilmaz BD, Sison C, et al. Endometriosis. *Endocr Rev*. 2019;40:1048-1079.
- Vannuccini S, Clemenza S, Rossi M, Petraglia F. Hormonal treatments for endometriosis: the endocrine background. *Rev Endocr Metab Disord*. 2022;23:333-355.
- Reis FM, Petraglia F, Taylor RN. Endometriosis: hormone regulation and clinical consequences of chemotaxis and apoptosis. *Hum Reprod Update*. 2013;19:406-418.
- Chapron C, Marcellin L, Borghese B, Santulli P. Rethinking mechanisms, diagnosis and management of endometriosis. *Nat Rev Endocrinol*. 2019;15:666-682.

7. Saunders PTK, Horne AW. Endometriosis: etiology, pathobiology, and therapeutic prospects. *Cell*. 2021;184:2807-2824.
8. Jiang L, Yan Y, Liu Z, Wang Y. Inflammation and endometriosis. *Front Biosci (Landmark ed)*. 2016;21:941-948.
9. Akoum A, Al-Akoum M, Lemay A, Maheux R, Leboeuf M. Imbalance in the peritoneal levels of interleukin 1 and its decoy inhibitory receptor type II in endometriosis women with infertility and pelvic pain. *Fertil Steril*. 2008;89:1618-1624.
10. Barcz E, Milewski Ł, Dziunycz P, Kamiński P, Płoski R, Malejczyk J. Peritoneal cytokines and adhesion formation in endometriosis: an inverse association with vascular endothelial growth factor concentration. *Fertil Steril*. 2012;97:1380-1386.e1.
11. Sikora J, Mielczarek-Palacz A, Kondera-Anasz Z. Association of the Precursor of interleukin-1 β and peritoneal inflammation-role in pathogenesis of endometriosis: proIL-1 β in endometriosis. *J Clin Lab Anal*. 2016;30:831-837.
12. Fan Y-Y, Chen H-Y, Chen W, Liu Y-N, Fu Y, Wang L-N. Expression of inflammatory cytokines in serum and peritoneal fluid from patients with different stages of endometriosis. *Gynecol Endocrinol*. 2018;34:507-512.
13. Carrarelli P, Luddi A, Funghi L, et al. Urocortin and corticotrophin-releasing hormone receptor type 2 mRNA are highly expressed in deep infiltrating endometriotic lesions. *Reprod Biomed Online*. 2016;33:476-483.
14. Hannun YA, Obeid LM. Sphingolipids and their metabolism in physiology and disease. *Nat Rev Mol Cell Biol*. 2018;19:175-191.
15. Maceyka M, Harikumar KB, Milstien S, Spiegel S. Sphingosine-1-phosphate signaling and its role in disease. *Trends Cell Biol*. 2012;22:50-60.
16. Blaho VA, Hla T. An update on the biology of sphingosine 1-phosphate receptors. *J Lipid Res*. 2014;55:1596-1608.
17. Bernacchioni C, Capezzuoli T, Vannuzzi V, et al. Sphingosine 1-phosphate receptors are dysregulated in endometriosis: possible implication in transforming growth factor β -induced fibrosis. *Fertil Steril*. 2021;115:501-511.
18. Santulli P, Marcellin L, Noël J-C, et al. Sphingosine pathway deregulation in endometriotic tissues. *Fertil Steril*. 2012;97:904-911.e5.
19. Ono Y, Kawakita T, Yoshino O, et al. Sphingosine 1-phosphate (S1P) in the peritoneal fluid skews M2 macrophage and contributes to the development of endometriosis. *Biomedicine*. 2021;9:1519.
20. Yoshino O, Yamada-Nomoto K, Kano K, et al. Sphingosine 1-phosphate (S1P) increased IL-6 expression and cell growth in endometriotic cells. *Reprod Sci*. 2019;26:1460-1467.
21. Rudzitis-Auth J, Christoffel A, Menger MD, Laschke MW. Targeting sphingosine kinase-1 with the low MW inhibitor SKI-5C suppresses the development of endometriotic lesions in mice. *Br J Pharmacol*. 2021;178:4104-4118.
22. Brinkmann V, Billich A, Baumruker T, et al. Fingolimod (FTY720): discovery and development of an oral drug to treat multiple sclerosis. *Nat Rev Drug Discov*. 2010;9:883-897.
23. Park S-J, Im D-S. Sphingosine 1-phosphate receptor modulators and drug discovery. *Biomol Ther (Seoul)*. 2017;25:80-90.
24. Drew BA, Burrow ME, Beckman BS. MEK5/ERK5 pathway: the first fifteen years. *Biochim Biophys Acta*. 2012;1825:37-48.
25. Obara Y, Nakahata N. The signaling pathway leading to extracellular signal-regulated kinase 5 (ERK5) activation via G-proteins and ERK5-dependent neurotrophic effects. *Mol Pharmacol*. 2010;77:10-16.
26. Goldsmith ZG, Dhanasekaran DN. G protein regulation of MAPK networks. *Oncogene*. 2007;26:3122-3142.
27. Paudel R, Fusi L, Schmidt M. The MEK5/ERK5 pathway in health and disease. *IJMS*. 2021;22:7594.
28. Stecca B, Rovida E. Impact of ERK5 on the hallmarks of cancer. *IJMS*. 2019;20:1426.
29. Diéguez-Martínez N, Espinosa-Gil S, Yoldi G, et al. The ERK5/NF- κ B signaling pathway targets endometrial cancer proliferation and survival. *Cell Mol Life Sci*. 2022;79:524.
30. Wang J, Erazo T, Ferguson FM, et al. Structural and atropisomeric factors governing the selectivity of Pyrimidobenzodiazepinones as inhibitors of kinases and bromodomains. *ACS Chem Biol*. 2018;13:2438-2448.
31. Williams CAM, Fernandez-Alonso R, Wang J, Toth R, Gray NS, Findlay GM. Erk5 is a key regulator of naive-primed transition and embryonic stem cell identity. *Cell Rep*. 2016;16:1820-1828.
32. Tusa I, Gagliardi S, Tubita A, et al. ERK5 is activated by oncogenic BRAF and promotes melanoma growth. *Oncogene*. 2018;37:2601-2614.
33. Sánchez-Fdez A, Re-Louhau MF, Rodríguez-Núñez P, et al. Clinical, genetic and pharmacological data support targeting the MEK5/ERK5 module in lung cancer. *NPJ Precis Oncol*. 2021;5:78.
34. Bruno M, Rizzo IM, Romero-Guevara R, et al. Sphingosine 1-phosphate signaling axis mediates fibroblast growth factor 2-induced proliferation and survival of murine auditory neuroblasts. *Biochim Biophys Acta Mol Cell Res*. 2017;1864:814-824.
35. Cencetti F, Bruno G, Blescia S, Bernacchioni C, Bruni P, Donati C. Lysophosphatidic acid stimulates cell migration of satellite cells. A role for the sphingosine kinase/sphingosine 1-phosphate axis. *FEBS J*. 2014;281:4467-4478.
36. Bernacchioni C, Ciarmela P, Vannuzzi V, et al. Sphingosine 1-phosphate signaling in uterine fibroids: implication in activin A pro-fibrotic effect. *Fertil Steril*. 2021;115:1576-1585.
37. Cencetti F, Bernacchioni C, Bruno M, et al. Sphingosine 1-phosphate-mediated activation of ezrin-radixin-moesin proteins contributes to cytoskeletal remodeling and changes of membrane properties in epithelial otic vesicle progenitors. *Biochim Biophys Acta Mol Cell Res*. 2019;1866:554-565.
38. Schmittgen TD, Livak KJ. Analyzing real-time PCR data by the comparative CT method. *Nat Protoc*. 2008;3:1101-1108.
39. Livak KJ, Schmittgen TD. Analysis of relative gene expression data using real-time quantitative PCR and the 2(-Delta Delta C(T)) method. *Methods*. 2001;25:402-408.
40. Tusa I, Menconi A, Tubita A, Rovida E. Pathophysiological impact of the MEK5/ERK5 pathway in oxidative stress. *Cell*. 2023;12:1154.
41. Kato Y, Tapping RI, Huang S, Watson MH, Ulevitch RJ, Lee JD. Bmk1/Erk5 is required for cell proliferation induced by epidermal growth factor. *Nature*. 1998;395:713-716.
42. Ranganathan A, Pearson GW, Chrestensen CA, Sturgill TW, Cobb MH. The MAP kinase ERK5 binds to and phosphorylates p90 RSK. *Arch Biochem Biophys*. 2006;449:8-16.
43. Kato Y, Zhao M, Morikawa A, et al. Big mitogen-activated kinase regulates multiple members of the MEF2 protein family. *J Biol Chem*. 2000;275:18534-18540.
44. Nincheri P, Bernacchioni C, Cencetti F, Donati C, Bruni P. Sphingosine kinase-1/S1P1 signalling axis negatively regulates mitogenic response elicited by PDGF in mouse myoblasts. *Cell Signal*. 2010;22:1688-1699.

45. Lin ECK, Amantea CM, Nomanbhoy TK, et al. ERK5 kinase activity is dispensable for cellular immune response and proliferation. *Proc Natl Acad Sci USA*. 2016;113:11865-11870.
46. Garcia JM, Vannuzzi V, Donati C, Bernacchioni C, Bruni P, Petraglia F. Endometriosis: cellular and molecular mechanisms leading to fibrosis. *Reprod Sci*. 2022;30:1453-1461.
47. Vannuccini S, Clifton VL, Fraser IS, et al. Infertility and reproductive disorders: impact of hormonal and inflammatory mechanisms on pregnancy outcome. *Hum Reprod Update*. 2016;22:104-115.
48. Tosti C, Pinzauti S, Santulli P, Chapron C, Petraglia F. Pathogenetic mechanisms of deep infiltrating endometriosis. *Reprod Sci*. 2015;22:1053-1059.
49. Scutiero G, Iannone P, Bernardi G, et al. Oxidative stress and endometriosis: a systematic review of the literature. *Oxid Med Cell Longev*. 2017;2017:7265238.
50. Clower L, Fleshman T, Geldenhuys WJ, Santanam N. Targeting oxidative stress involved in endometriosis and its pain. *Biomolecules*. 2022;12:1055.
51. Huang W-C, Nagahashi M, Terracina KP, Takabe K. Emerging role of Sphingosine-1-phosphate in inflammation, cancer, and Lymphangiogenesis. *Biomolecules*. 2013;3:408-434.
52. Lin C-C, Yang C-C, Cho R-L, Wang C-Y, Hsiao L-D, Yang C-M. Sphingosine 1-phosphate-induced ICAM-1 expression via NADPH oxidase/ROS-dependent NF- κ B cascade on human pulmonary alveolar epithelial cells. *Front Pharmacol*. 2016;7:80.
53. Lee C-H, Choi JW. S1P/S1P2 signaling Axis regulates both NLRP3 upregulation and NLRP3 inflammasome activation in macrophages primed with lipopolysaccharide. *Antioxidants (Basel)*. 2021;10:1706.
54. Rapizzi E, Taddei ML, Fiaschi T, Donati C, Bruni P, Chiarugi P. Sphingosine 1-phosphate increases glucose uptake through trans-activation of insulin receptor. *Cell Mol Life Sci*. 2009;66:3207-3218.
55. Yoshino O, Osuga Y, Hirota Y, et al. Possible pathophysiological roles of mitogen-activated protein kinases (MAPKs) in endometriosis. *Am J Reprod Immunol*. 2004;52:306-311.
56. Ahn SH, Khalaj K, Young SL, Lessey BA, Koti M, Tayade C. Immune-inflammation gene signatures in endometriosis patients. *Fertil Steril*. 2016;106:1420-1431.e7.
57. Bora G, Yaba A. The role of mitogen-activated protein kinase signaling pathway in endometriosis. *J Obstet Gynaecol Res*. 2021;47:1610-1623.
58. Abe J, Kusuhara M, Ulevitch RJ, Berk BC, Lee JD. Big mitogen-activated protein kinase 1 (BMK1) is a redox-sensitive kinase. *J Biol Chem*. 1996;271:16586-16590.
59. Yang M, Cooley BC, Li W, et al. Platelet CD36 promotes thrombosis by activating redox sensor ERK5 in hyperlipidemic conditions. *Blood*. 2017;129:2917-2927.
60. Khan AUH, Allende-Vega N, Gitenay D, et al. Mitochondrial complex I activity signals antioxidant response through ERK5. *Sci Rep*. 2018;8:7420.
61. García-Hoz C, Sánchez-Fernández G, Díaz-Meco MT, Moscat J, Mayor F, Ribas C. G α q acts as an adaptor protein in protein kinase C ζ (PKC ζ)-mediated ERK5 activation by G protein-coupled receptors (GPCR). *J Biol Chem*. 2010;285:13480-13489.
62. Barra V, Kuhn A-M, von Knethen A, Weigert A, Brüne B. Apoptotic cell-derived factors induce arginase II expression in murine macrophages by activating ERK5/CREB. *Cell Mol Life Sci*. 2011;68:1815-1827.
63. Fernández-Pisonero I, Dueñas AI, Barreiro O, Montero O, Sánchez-Madrid F, García-Rodríguez C. Lipopolysaccharide and Sphingosine-1-phosphate cooperate to induce inflammatory molecules and leukocyte adhesion in endothelial cells. *J Immunol*. 2012;189:5402-5410.
64. Lee H, Deng J, Kujawski M, et al. STAT3-induced S1PR1 expression is crucial for persistent STAT3 activation in tumors. *Nat Med*. 2010;16:1421-1428.
65. Campos LS, Rodriguez YI, Leopoldino AM, et al. Filamin a expression negatively regulates sphingosine-1-phosphate-induced NF- κ B activation in melanoma cells by inhibition of Akt signaling. *Mol Cell Biol*. 2016;36:320-329.
66. Hsu C-K, Lee I-T, Lin C-C, Hsiao L-D, Yang C-M. Sphingosine-1-phosphate mediates COX-2 expression and PGE2/IL-6 secretion via c-Src-dependent AP-1 activation. *J Cell Physiol*. 2015;230:702-715.
67. Abe JI, Takahashi M, Ishida M, Lee JD, Berk BC. c-Src is required for oxidative stress-mediated activation of big mitogen-activated protein kinase 1. *J Biol Chem*. 1997;272:20389-20394.
68. Zhao J, Kyotani Y, Itoh S, Nakayama H, Isosaki M, Yoshizumi M. Big mitogen-activated protein kinase 1 protects cultured rat aortic smooth muscle cells from oxidative damage. *J Pharmacol Sci*. 2011;116:173-180.
69. Lee JD, Ulevitch RJ, Han J. Primary structure of BMK1: a new mammalian map kinase. *Biochem Biophys Res Commun*. 1995;213:715-724.
70. Honda T, Obara Y, Yamauchi A, et al. Phosphorylation of ERK5 on Thr732 is associated with ERK5 nuclear localization and ERK5-dependent transcription. *PLOS One*. 2015;10:e0117914.
71. Machairiotis N, Vasilakaki S, Thomakos N. Inflammatory mediators and pain in endometriosis: a systematic review. *Biomedicine*. 2021;9:54.
72. Martínez S, Garrido N, Coperias JL, et al. Serum interleukin-6 levels are elevated in women with minimal-mild endometriosis. *Hum Reprod*. 2007;22:836-842.
73. De Andrade VT, Năcul AP, Dos Santos BR, Lecke SB, Spritzer PM, Morsch DM. Circulating and peritoneal fluid interleukin-6 levels and gene expression in pelvic endometriosis. *Exp Ther Med*. 2017;14:2317-2322.
74. Mu F, Harris HR, Rich-Edwards JW, et al. A prospective study of inflammatory markers and risk of endometriosis. *Am J Epidemiol*. 2018;187:515-522.
75. Ren K, Torres R. Role of interleukin-1beta during pain and inflammation. *Brain Res Rev*. 2009;60:57-64.

SUPPORTING INFORMATION

Additional supporting information can be found online in the Supporting Information section at the end of this article.

How to cite this article: Seidita I, Tusa I, Prisinzano M, et al. Sphingosine 1-phosphate elicits a ROS-mediated proinflammatory response in human endometrial stromal cells via ERK5 activation. *The FASEB Journal*. 2023;37:e23061. doi:[10.1096/fj.202300323R](https://doi.org/10.1096/fj.202300323R)